[CANCER RESEARCH 63, 2462–2469, May 15, 2003]

Use of a Vaccine Strain of Measles Virus Genetically Engineered to Produce Carcinoembryonic Antigen as a Novel Therapeutic Agent against Glioblastoma Multiforme[1]

Loi K. Phuong, Cory Allen, Kah-Whye Peng, Caterina Giannini, Suzanne Greiner, Cynthia J. TenEyck, Prasanna K. Mishra, Slobodan I. Macura, Stephen J. Russell, and Evanthia C. Galanis[2]

Departments of Neurosurgery [L. K. P.], Molecular Medicine [C. A., K. W. P., S. G., C. J. T., S. R., E. G.], Pathology [C. G.], Biochemistry and Molecular Biology [P. M., S. I. M.], and Oncology [E. G.], Mayo Clinic, Rochester, Minnesota 55905

ABSTRACT

Despite the most aggressive medical and surgical treatments, glioblastoma multiforme remains incurable with a median survival of <1 year. We investigated the antitumor potential of a novel viral agent, an attenuated strain of measles virus (MV), derived from the Edmonston vaccine lineage, genetically engineered to produce carcinoembryonic antigen (CEA). CEA production as the virus replicates can serve as a marker of viral gene expression. Infection of a variety of glioblastoma cell lines including U87, U118, and U251 at MOIs 0.1, 1, and 10 resulted in significant cytopathic effect consisting of excessive syncycial formation and massive cell death at 72–96 h from infection. terminal deoxynucleotidyltransferase-mediated nick end labeling assays demonstrated the mechanism of cell death to be predominantly apoptotic. The efficacy of this approach *in vivo* was examined in BALB/c nude mice by using both s.c. and intracranial orthotopic U87 tumor models. In the s.c. U87 model, mice with established xenografts were treated with a total dose of 8×10^7 plaque forming units of MV-CEA, administered i.v. Mice treated with UV light inactivated MV, and untreated mice with established U87 tumors were used as controls. There was statistically significant regression of s.c. tumors ($P < 0.001$) and prolongation of survival ($P = 0.007$) in MV-CEA treated animals compared with the two control groups. In the intracranial orthotopic U87 model, there was significant regression of intracranial U87 tumors treated with intratumoral administration of MV-CEA at a total dose of 1.8×10^6 plaque forming units as assessed by magnetic resonance image ($P = 0.002$), and statistically significant prolongation of survival as compared with mice that received UV-inactivated virus and untreated mice ($P = 0.02$). Histological examination of brains of MV-CEA-treated animals revealed complete regression of the tumor with the presence of a residual glial scar and reactive changes, mainly presence of hemosiderin-laden macrophages. In addition, CEA levels in the peripheral blood in both the s.c. and orthotopic models increased before tumor regression, indicating viral gene expression, and returned to normal when the tumors regressed. Ifnar^{ko} CD46 Ge transgenic mice, susceptible to MV infection, were used to assess central nervous system toxicity of MV-CEA. Intracranial administration of MV-CEA into the caudate nucleus of Ifnar^{ko} CD46 Ge did not result in clinical neurotoxicity. Pathologic examination demonstrated limited microglial infiltration surrounding the injection site. In summary, MV-CEA has potent antitumor activity against gliomas *in vitro*, as well as in both s.c. and orthotopic U87 animal models. Monitoring CEA levels in the serum can serve as a low-risk method of detecting viral gene expression during treatment, and could allow dose optimization and individualization of treatment.

INTRODUCTION

Glioblastoma multiforme is the most frequent primary brain tumor in adults and accounts for the majority of 18,500 primary brain tumor cases diagnosed each year in the United States (1). It is one of the most lethal malignancies with a median survival of <1 year despite multimodality treatment including surgery, chemotherapy, and radiation therapy. Gliomas represent a promising target for gene transfer approaches given their limited ability to metastasize. Although the first clinical gene transfer trial in brain tumors was conducted in the early 1990s, significant clinical benefit has not been realized to date (2–5).

Our laboratory has demonstrated previously the antitumor potential of the MV[3] F and H fusogenic membrane glycoproteins against gliomas using nonreplicating adenoviral vectors encoding the F and H proteins in U87 subcutaneous xenografts (6). However, one of the main challenges associated with use of nonreplicating vectors in clinical gene transfer approaches is their limited transduction efficacy. In a trial of IT administration of a nonreplicating p53 adenovirus in recurrent glioma patients, transgene expression was found only in a short distance (5–8 mm) from the injection site (7), thus pointing to the limitations associated with clinical application of nonreplicating vectors for treatment of brain tumors. Therefore, to additionally develop the MV fusogenic F and H proteins as antitumor agents against gliomas, we chose to use the natural carrier of these proteins, *i.e.*, a replicating attenuated vaccine strain of MV.

MV is a negative strand RNA paramyxovirus. The virus exerts its CPE by formation of multinuclear cell aggregates, *i.e.*, syncytia, resulting from fusion of infected cells (8). MV enters the cells via interaction of the H glycoprotein with the MV receptors SLAM (being predominantly present in B- and T- lymphocytes; Ref. 9) and CD46 (10, 11). The MV receptor CD46, or membrane cofactor protein, belongs to the family of membrane-associated complement regulatory proteins, which serve as an important mechanism of self-protection against complement-mediated lysis. CD46 is frequently overexpressed on tumors (12). In contrast to wild-type MV that can cause potentially serious disease, vaccine strains of MV have an excellent safety record with millions of vaccine doses having been administered and have significantly decreased the measles incidence, morbidity, and mortality worldwide (13).

Antitumor activity of attenuated strains of the Edmonston vaccine lineage has been demonstrated in lymphoma, multiple myeloma, and ovarian cancer models (14–16). It is of note that whereas the wild-type MV enters more efficiently through the SLAM receptor, the Edmonston vaccine strain of MV enters cells predominantly through CD46 receptor (17). Schneider *et al.* (18) have shown that MV with wild-type H protein enters cells through SLAM two to three times more efficiently than MV with the H protein of an attenuated Edmonston strain. In contrast, cell entry efficiency through CD46 was lower

Received 10/28/02; accepted 3/12/03.

The costs of publication of this article were defrayed in part by the payment of page charges. This article must therefore be hereby marked *advertisement* in accordance with 18 U.S.C. Section 1734 solely to indicate this fact.

[1] Supported by NIH CA 84388 (to E. G.) and by a grant from the Fraternal Order of Eagles.

[2] To whom requests for reprints should be addressed, at Department of Oncology, Mayo Clinic, 200 First Street SW, Rochester, MN 55905. Phone: (507) 284-3731; Fax: (507) 538-0823; E-mail: galanis.evanthia@mayo.edu.

[3] The abbreviations used are: MV, measles virus, CEA, carcinoembryonic antigen; H, hemagglutinin; N, nucleocapsid; CPE, cytopathic effect; MOI, multiplicity of infection; TUNEL, terminal deoxynucleotidyltransferase-mediated nick end labeling; pfu, plaque-forming unit(s); MRI, magnetic resonance imaging; IT, intratumoral; HSV, herpes simplex virus; PET, positron emission tomography; SPECT, single photon emission computed tomography; [^{124}I]-FIAU, ^{124}I-labeled 2′-fluoro-2′-deoxy-1B-D-arabino-furanosyl-5-iodo-uracil.

for the MV expressing wild-type H protein. These differences were amplified at the cell fusion stage because the wild-type H protein failed to fuse CD46-expressing cells (18). This property can in part explain the antitumor properties of the virus, given the frequent CD46 overexpression in tumors. In contrast, the wild-type MV enters peripheral blood mononuclear cells much more efficiently as compared with the measles Edmonston strain of the vaccine lineage; 24 h after infection, ~30% of the peripheral blood monocytes were infected by the MV expressing the wild-type H protein as compared with <4% of the monocytes infected by an Edmonston strain of the vaccine lineage (18). This observation, also confirmed by Peng *et al.* (15), points to a favorable toxicity profile for the Edmonston vaccine strain.

However, the challenge when trying to translate this antitumor potential in a brain tumor model was to devise a system whereby viral gene expression could be tracked *in vivo*, and subsequently dosing and administration schedule could be optimized without resorting to histological tissue analysis. This is crucial if the treatment is to be translated in brain tumor patients, because repeat brain biopsies to assess viral gene expression can have significant associated risks and are not ethically justified. Engineering the vaccine strain of MV to express a marker peptide that can be easily detected in the serum represents a potential answer to this problem. For this purpose we chose the human CEA, a marker peptide not produced by gliomas. Therefore, its detection in our model could only be associated with viral gene expression. CEA is a 180 K_d glycoprotein, and it represents one of the best characterized tumor marker antigens in terms of tissue distribution and molecular structure (19). CEA is expressed in the vast majority of colorectal, gastric, and pancreatic carcinomas, as well as in ~50% of breast cancer and 70% of non-small cell lung cancer specimens. However, it is not expressed in gliomas, and in its secreted form does not have known biological activity. CEA is not sufficiently immunogenic on its own, and little evidence exists for humoral or cell-mediated immunity to CEA in cancer patients (19).

A recombinant Edmonston strain of MV that expresses the soluble extracellular N-terminal domain of human CEA, MV-CEA, was generated (20). In this study we evaluated the efficacy of MV-CEA against glioblastoma multiforme *in vitro* and *in vivo* using murine subcutaneous and orthotopic intracranial models. We have demonstrated potent antitumor efficacy associated with apoptotic cell death. Furthermore, serum CEA levels in the treated mice could serve as a good correlate of viral gene expression. No clinical neurotoxicity and no significant pathology were observed after intracranial administration of MV-CEA in transgenic mice susceptible to MV infection ($Ifnar^{ko}$ CD46 Ge), thus pointing toward the safety of the approach.

MATERIALS AND METHODS

Cell Culture. Vero (African green monkey) cell line and human malignant glioma cell lines U87, U251, and U118 were obtained from American Type Culture Collection (Manassas, VA). They were grown in DMEM supplemented with 5% and 10% FCS, respectively.

Production of MV. The construction of MV-CEA has been described elsewhere (20). In summary, a c-DNA infectious clone derived from the Edmonston vaccine lineage (21) was engineered by inserting the human CEA gene upstream from the MV *N* gene (Fig. 1). The virus was propagated by infecting 1.5×10^6 Vero cells in T75 flasks at a MOI of 0.05 in 3 ml Opti-MEM (Life Technologies, Inc.) at 37°C for 2 h. The medium was then replaced with DMEM (Life Technologies, Inc.). The cells were incubated at 37°C for 2 days and then transferred to 32°C for 1 day, and subsequently harvested in 1 ml Opti-MEM (Life Technologies, Inc.). The virus was released by two cycles of freezing and thawing. The titer of the virus was determined by 50% end point dilution assay on Vero cells in a 96-well plate (22, 23).

Fig. 1. Schematic representation of MV-CEA. The cDNA encoding for the human CEA was inserted upstream of the *N* gene. *P*, phosphoprotein gene; *M*, matrix protein gene; *F*, fusion protein gene; *L*, large protein gene (adapted with permission from Peng *et al.*, Ref. 20).

Preparation of inactivated MV-CEA followed the same procedures as described above. The virus was inactivated by exposure to UV light at 120,000 $\mu J/cm^2$ for 30 min. Confirmation of virus inactivation was made by titration on Vero cells.

Assessment of the CPE *in Vitro*. To determine the CPE of MV-CEA, cells were plated in six-well plates at a density of 10^5 cells/well. Twenty-four h after seeding, the cells were infected with MV-CEA at different MOIs from 0.1, 1, and 10 in 1 ml of Opti-MEM for 2 h at 37°C. At the end of the incubation period, the virus was removed and the cells were maintained in their standard medium. The same number of uninfected cells in six-well plates were used as controls. The number of viable cells in each well was counted using a hemocytometer at 24, 48, 72, 96, 120, and 144 h after infection. Viable cells were identified using trypan blue staining. The percentage of surviving cells was calculated by dividing the number of viable cells in the infected well by the number of viable cells in the uninfected well corresponding to the same time point. In addition, two wells per cell line and time point were fixed with 0.5% glutaraldehyde stained with crystal violet to better illustrate the observed CPE.

Assessment of MV-CEA Replication in Glioma Cell Lines. U87 and U251 cells were plated in six-well plates at a density of 10^5 cells/well at a MOI of 1.0. The cells were infected as described above and harvested at 24, 48, and 72 h. The viruses were released by two cycles of freezing/thawing. The viral titer was determined by 50% end point dilution assay on Vero cells in a 96-well plate as described above.

CEA Level Determination in the Supernatant of MV-CEA-infected Cells. U87 or U251 cells were plated in six-well plates at a density of 10^5 cells/well. Twenty-four h later, the cells were infected with MV-CEA at a MOI of 1.0. The medium was changed every 24 h to track the daily production in cell supernatant CEA in each 24-h period for 3 days. The CEA level at 24, 48, and 72 h after infection was measured using the Bayer Centaur Immunoassay System (Bayer, Tarrytown, NY). Uninfected cell supernatants at the same time points were used as negative controls.

Assessment of Apoptosis by TUNEL Assay. U87, U118, and U251 glioblastoma cell lines were plated on two well culture slides (Becton Dickinson, Franklin Lakes, NJ) at a density of 1×10^5 cells per well. Cells were infected in duplicate with MV-CEA at an MOI of 1 the following day. Cells were analyzed for the presence of apoptosis using the *In Situ* Cell Death Detection kit, Fluorescein (Roche, Mannheim, Germany) 2, 4, and 6 days after infection. Air-dried cells were fixed with 4% paraformaldehyde, washed with PBS, permeabilized with 0.1% Triton X-100 in 0.1% sodium citrate, and incubated with TUNEL reaction mixture (consisting of calf thymus terminal deoxynucleotidyltransferase and nucleotide mixture in reaction buffer) for 60 min at 37°C. Apoptotic cells were visualized by fluorescence microscopy. Infected cells treated with reaction mixture, from which terminal deoxynucleotidyltransferase was omitted, were used as negative control. Noninfected cells, exposed to DNase I for 10 min before the addition of the TUNEL reaction mixture, were used as positive controls.

Determination of CD46 Expression by Flow Cytometry. Cells were harvested, washed in 2% BSA-PBS, incubated with mouse antihuman CD46 antibody (PharMingen, San Diego, CA) for 1 h on ice, washed, and subsequently incubated with FITC-conjugated antimouse antibody (Sigma Chemical Co., St. Louis, MO) for 1 h on ice. Samples were assayed on a Becton-Dickinson FACScan Plus cytometer. Analysis was performed using the CellQuest software (Becton-Dickinson, San Jose, CA).

Animal Experiments. The experimental protocols were approved by the Mayo Clinic Institutional Animal Care and Use Committee.

Subcutaneous U87 Tumor Model. Six $\times$ 10^6 U87 cells in PBS were injected subcutaneously into the right flanks of 4-week-old BALB/c nude mice using a 27-gauge needle. The mice were examined daily for tumor growth. The length and width of the tumors were measured with a caliper. Tumor volume was calculated as length $\times$ $width^2/2$ (24). The mice were randomly assigned into one of three groups: i.v. administration of MV-CEA ($n = 8$), i.v. administration of UV-inactivated MV-CEA ($n = 8$), or untreated ($n = 7$). i.v. administration of MV-CEA or UV inactivated MV-CEA (10^7 pfu/200 μl) was

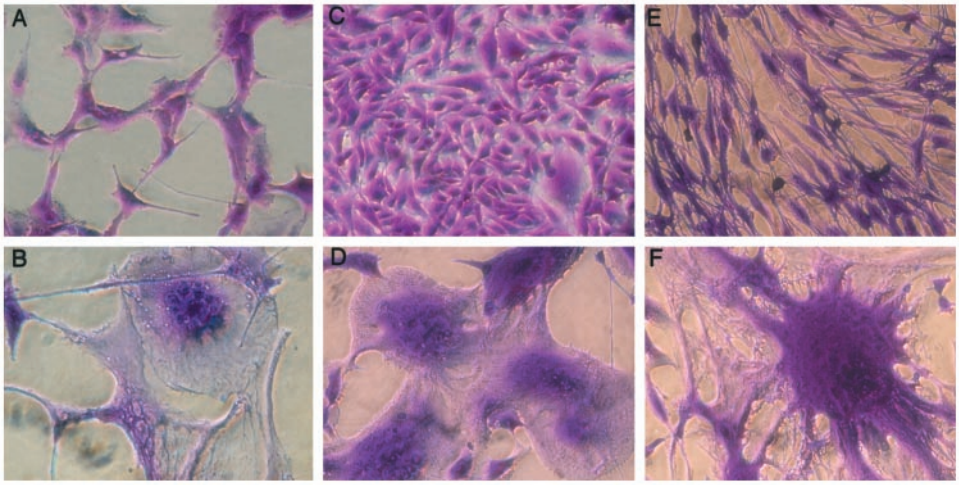

Fig. 2. *A–F*, MV-CEA infection results in prominent syncytia formation in U87, U251, and U118 cells. Crystal violet stain, (×200 magnification). *A, C,* and *E,* uninfected U87, U251, and U118 cells, respectively. *B, D,* and *F*, 72 h after infection of U87, U251, and U118 cells, respectively, with MV-CEA (MOI 1.0). Extensive syncytia formation is observed preceding cell death.

initiated 4 days after tumor cell implantation when the average tumor volume was 10 mm^3. Treatments were repeated every other day for a total of eight doses (total dose of 8×10^7 pfu) over an 18-day period. Weekly venous blood draws (0.2 ml/10 g body weight) from mice that received MV-CEA or UV inactivated MV-CEA were started at 3 days after treatment initiation to determine serum CEA level. Animals were euthanized if weight loss >20% of body weight was observed or the tumor diameter exceeded 1 cm.

***In Situ* Hybridization for MV-CEA N mRNA.** U87 subcutaneous tumors were harvested and fixed in 10% formalin. The tissue was paraffin embedded and sectioned at 5 μm thickness. The sections were then deparaffinized. A digoxigenin-labeled N RNA of negative polarity was used to probe for the presence of MV N mRNA as described previously (15).

Intracranial Orthotopic Tumor Model. Injection of U87 cells into the right caudate nucleus of 4-week-old BALB/c mice was performed using the small animal stereotactic frame (ASI Instruments). The injection coordinates were 1.5 mm anterior to the coronal suture, 2.5 mm to the right of the sagittal suture, and 3.5 mm below the skull surface. U87 cells (10^6) in PBS were injected over 7 min using a 26-gauge Hamilton syringe under i.p. ketamine/xylazine anesthesia.

Confirmation of successful tumor implantation was done 3 days later with MRI using a Bruker DRX-300 (300 Mhz 1H) widebore two channel multinuclear spectrometer (Biospin, Billerica, MA). The MRI was performed 5 min after i.p. administration of gadolinium at a dose of 0.1 mmol/kg. The mice were randomly assigned into one of three groups: IT administration of MV-CEA ($n = 8$), IT administration of UV-inactivated MV-CEA ($n = 7$), or untreated ($n = 7$). IT injection of MV-CEA or UV-inactivated MV-CEA (3×10^5 pfu/10 μl) was performed using the same coordinates on the stereotactic frame, as for tumor cell implantation. The treatments were repeated every other day for a total of six doses (1.8×10^6 pfu) over a 12-day period. Another MRI with i.p. gadolinium administration was done after completion of treatments at 21 days after implantation of tumor cells. Weekly venous blood draws (0.2 ml/10 g body weight) from mice that received MV-CEA or UV-inactivated MV-CEA were started at 3 days after treatment initiation to determine serum CEA level. The animals were euthanized if they developed neurological deficits such as hemiparesis or lethargy, or if weight loss >20% of body weight occurred. Volumetric measurements of the intracranial tumors were obtained with MRI, using the region of interest method in Analyze 3.1 (Mayo Clinic).

Determination of CEA *in Vivo*. Blood samples from treated and control animals were collected as described above. CEA levels were measured using the Bayer Centaur Immunoassay System.

Statistical Analysis. Statistical analysis of tumor volumes before and after treatment among the groups was done using repeated measures ANOVA (25). The survival of mice in each of the treatment groups in the s.c. and intracranial models was compared using the log-rank test. A P of <0.05 was considered statistically significant.

Assessment of MV-CEA Toxicity in an $Ifnar^{ko}$ CD46 Ge Mouse Model. Rodent cells normally do not express the MV CD46 or SLAM receptors; therefore, the animal models we used to assess efficacy do not allow us to adequately evaluate toxicity of MV-CEA. For this purpose we performed a pilot toxicity study using a transgenic mouse model that expresses CD46 and lacks the IFN-$\alpha\beta$ receptor. The model was kindly provided by Dr. Roberto Cattaneo (Mayo Clinic, Rochester, MN) and was obtained by insertion of a yeast artificial chromosome containing human CD46 receptor and knockout of the IFN-$\alpha\beta$ receptor ($Ifnar^{ko}$ CD46 Ge; Ref. 26). CD46 expression in the brain of CD46 Ge mice examined by Western immunoblotting has been shown to be comparable with CD46 expression in human brain (26). These mice are susceptible to MV-Edm infection, when the virus is administered via the intranasal, intracerebral, i.p., and i.v. routes (27, 28). Mice recover from infection, with robust anti-MV antibody titers detected by ELISA by day 14 and 28 (29).

For the pilot toxicity study, we used the same parameters for stereotactic injection of MV-CEA, and same viral dose and volume of administration as for the efficacy study described above. $Ifnar^{ko}$-CD46 Ge transgenic mice were injected stereotactically with a total dose of 1.8×10^6 pfu of either MV-CEA (7 animals), or UV-inactivated MV-CEA (2 animals) or normal saline (2 animals) over the course of six injections during a 2-week period. Blood was collected from each animal for serum CEA levels starting 1 week after the first injection and every week thereafter until the day of sacrifice. Mice were followed clinically on a daily basis. The mice were euthanized on days 2–4, 14, and 21 after last injection to assess acute, subacute, and late toxicity. The brains of the animals were perfused with 5% buffered paraformaldehyde and subjected to pathologic examination by a neuropathologist (C. G.).

RESULTS

MV-CEA Replicates and Causes Significant CPE in Glioma Cells. FACS analysis confirmed that the glioma cell lines express abundant CD46, with U251 having the most prominent CD46 expres-

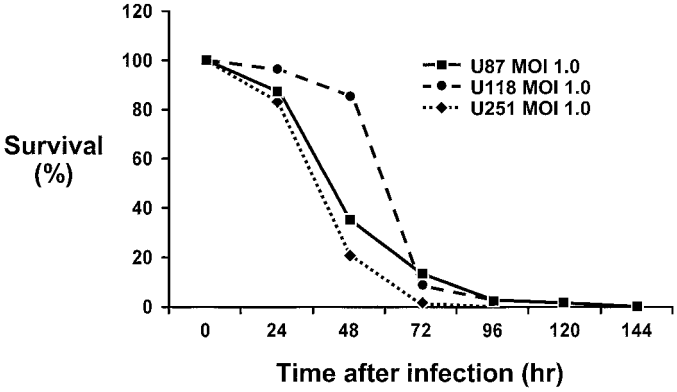

Fig. 3. CPE of MV-CEA (MOI 1.0) on U87, U251, and U118 cells at MOI 1.0. Cell viability is determined by trypan blue exclusion. Less than 1% of the cells are viable by 120 h after infection.

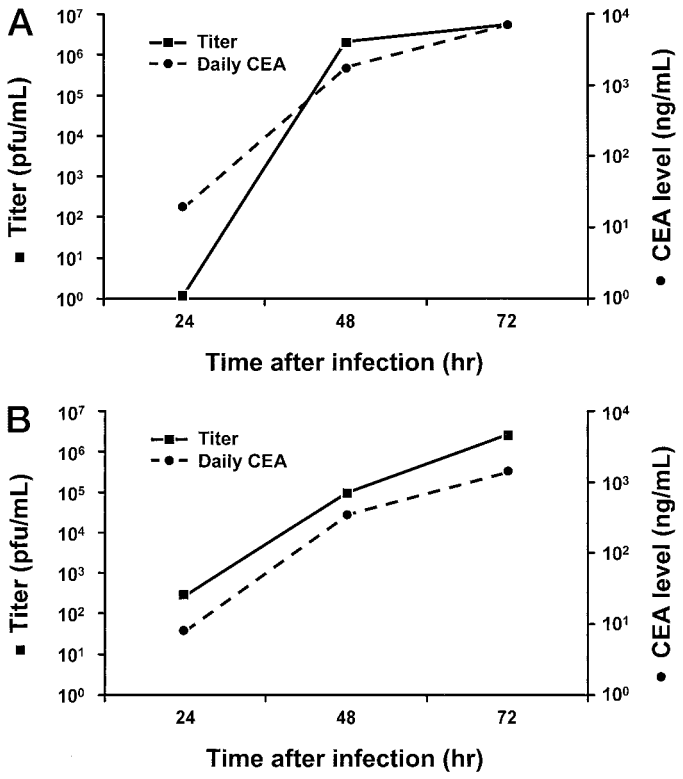

Fig. 4. Replication of MV-CEA in U87 (*A*) and U251 (*B*) cells is demonstrated by the titers obtained at 24, 48, and 72 h after infection at MOI of 1.0. Titration was done on Vero cells in a 96-well plate using the 50% end dilution method. The rise in MV-CEA titer correlated with increasing CEA titers in the cell supernatant, thus indicating that CEA levels represent a good marker of viral gene expression/propagation.

sion, followed by U87 and U118 (data not shown). Prominent syncytia formation and CPE was seen after infection of all three of the glioma cell lines with MV-CEA (Fig. 2, *A–F*). At an MOI as low as 1, in all three of the glioma cell lines, cell death was observed in >90% of cells by 72 h (Fig. 3). Less than 1% of the cells were viable by 120 h after infection. Differences at the level of CD46 overexpression did not translate in differences in the antitumor effect, indicating that the observed CD46 levels were adequate in order for massive cell-cell fusion and death to occur.

To determine whether MV-CEA could replicate in glioma cells, titers of the virus from those cells were obtained 24, 48, and 72 h after infection. As shown in Fig. 4, *A* and *B*, the malignant glioma cell lines supported robust replication of MV-CEA. The increase in titer was associated with a significant rise in the CEA level in the culture supernatants that correlated with viral replication/gene expression. The CEA levels in uninfected glioma cells were undetectable.

The Mechanism of Cell Death in Measles-induced Syncytia Is Predominantly Apoptotic. To investigate the mechanism of cell death, we performed TUNEL assays in time course experiments using all three of the glioma cell lines. The mechanism of cell death was predominantly apoptotic. Early after infection (day 2), syncytia were TUNEL-negative (Fig. 5*B*). By day 4 the nuclear clusters in some syncytia became brightly positive and others weakly positive by TUNEL staining (Fig. 5*D*). Overall, ~50% of syncytia showed TUNEL-positive nuclear staining at this time point, and the cytoplasm was invariably negative. By day 6 after infection, the nuclear pattern of TUNEL positivity had given way to positive diffuse staining throughout the cytoplasm, with residual positive nuclei and nuclear fragments (Fig. 5*F*).

MV-CEA Has Potent Antitumor Effect When Administered i.v. in BALB/c Nude Mice Bearing U87 Xenografts. The antitumor effect MV-CEA was assessed in established subcutaneous U87 glioma xenografts in BALB/c nude mice. As shown in Fig. 6*A*, mice treated by i.v. injection of MV-CEA (total dose of 8×10^7 pfu) had significant tumor regression at completion of treatment as compared with mice treated with the same dose of UV-inactivated MV-CEA or untreated mice ($P < 0.001$). Specifically, complete regression of the subcutaneous tumors was seen in all of the 8 mice treated with i.v. MV-CEA. As shown in Fig. 6*B*, there was a statistically significant prolongation of survival for mice treated with i.v. MV-CEA ($P = 0.007$). The median survival of MV-CEA-treated mice was 83 days, as compared with 35 and 29 days in the mice treated with UV-inactivated MV-CEA and untreated mice, respectively.

To confirm MV-CEA tumor infection after i.v. administration of MV-CEA in the subcutaneous U87 tumor model we performed *in situ* hybridization for MV N mRNA on tumor sections from a mouse treated with i.v. MV-CEA and an UV-inactivated MV-CEA-treated control mouse. Scattered foci of positive staining were observed in the tumor deriving from the MV-CEA-treated mouse, indicating the presence of viral mRNA within the tumor (data not shown). Given the fact that all of the tumors in the MV-CEA-treated group regressed completely, the presence of only scattered foci of positive staining for MV N mRNA indicates that a bystander effect is also likely contributing to tumor eradication. No staining was observed in the control tumor.

Serum CEA Profiles Correlate with the Antitumor Effect. Serum CEA levels started increased in the mice treated with the MV-

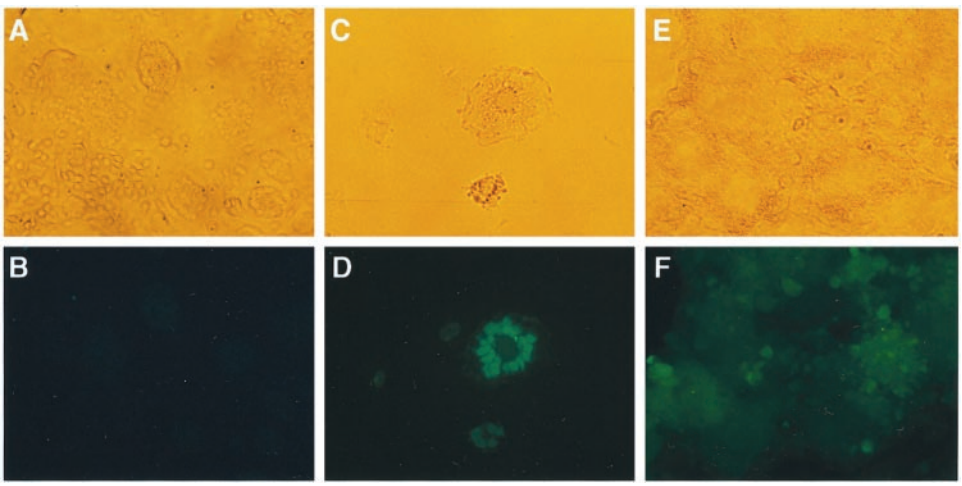

Fig. 5. TUNEL assay of U251 cells infected with MV-CEA at an MOI of 1, at 2 days (*A* and *B*), 4 days (*C* and D), and 6 days (*E* and *F*) after infection with MV-CEA. There is significant increase in the number of apoptotic (*green fluorescent*) nuclei per syncytia and the number of apoptotic syncytia preceding syncytial death on days 4 and 6 (×200 magnification).

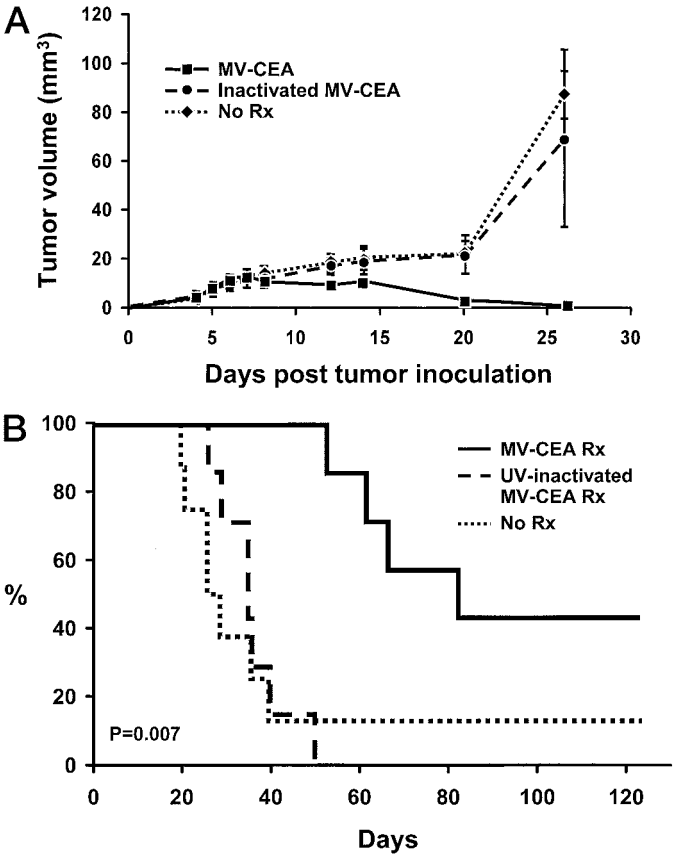

Fig. 6. *A*, antitumor effect of MV-CEA, administered i.v. in a subcutaneous U87 model. U87 gliomas were established in the right flank of female BALB/c nude mice (7–8 mice/group). Four days after tumor implantation the mice received i.v. 10^7 pfu of MV-CEA for a total of eight doses (group 1) or same dose of UV inactivated MV-CEA (group 2). Group 3 remained untreated. The mice had similar tumor volumes before treatment ($P = 0.45$). All mice treated with i.v. MV-CEA had complete tumor regression in contrast to the UV-inactivated MV-CEA and untreated mice ($P < 0.001$). The plot was censored at 26 days because of deaths occurring in the two control groups. *B*, mice treated with i.v. MV-CEA had significantly longer survival than mice that received UV-inactivated MV-CEA or no treatment ($P = 0.007$).

CEA by day 3 after treatment was initiated. It peaked at 10 days and then gradually declined to baseline level. The CEA levels in the mice treated with UV-inactivated virus or untreated mice remained undetectable. To determine the correlation between serum CEA and tumor volume, a plot of the mean CEA level was superimposed on the mean tumor volume of mice treated with MV-CEA (Fig. 7). The growth and regression of the tumor paralleled the rise and fall of the serum CEA level.

MV-CEA Has Potent Antitumor Effect When Administered Intratumorally in Established Intracranial U87 Glioma Xenografts in BALB/c Nude Mice. To assess the antitumor effect of MV-CEA in a model that more closely resembles disease in humans, we established intracranial U87 xenografts in BALB/c nude mice. The intracranial tumor volumes as measured with MRI, obtained 3 days after tumor implantation and before initiating treatment, were similar among the three groups ($P = 0.28$). There was significant regression of the intracranial tumors after IT administration of MV-CEA (3×10^5 pfu/dose for 6 doses, total dose of 1.8×10^6 pfu) as compared with mice that received the same dose of UV-inactivated MV-CEA or no treatment ($P = 0.0028$; Fig. 8*A*). Seven of the 8 mice that received MV-CEA had complete regression of the tumor based on MRI. Tumor regrowth was subsequently observed in some of the treated animals, but despite that, mice treated with IT MV-CEA had significantly longer survival than mice receiving UV-inactivated MV-CEA or no treatment ($P = 0.02$; Fig. 8*B*). Approximately 60% of the MV-CEA-treated mice remained alive and tumor-free at 80 days from tumor inoculation (Fig. 8*B*). Although the tumor volumes were much smaller than in the subcutaneous model, 5 of the 8 mice treated with IT MV-CEA had elevated serum CEA levels that returned to normal at the completion of treatment when tumor regression was observed in MRI. The mice that received UV-inactivated MV-CEA or no treatment had undetectable serum CEA levels.

Fig. 9, *A* and *B*, depicts a brain MRI from a mouse in the MV-CEA-treated group, before (Fig. 9*A*) and 18 days after (Fig. 9*B*) initiation of IT treatment with MV-CEA. Autopsy of the mouse revealed pathologic complete tumor regression. No tumor cells were seen in the examination of the brain (Fig. 9*C*). Reactive changes and hemosiderin-laden macrophages were present in the injection site (Fig. 9*C*, *arrow*). In contrast, the continuous growth of the intracranial tumor in a mouse that received UV-inactivated MV-CEA intratumorally, as depicted in consecutive brain MRIs, is demonstrated in Fig. 9, *D* and *E*. On histological examination, the intracranial tumor was hypercellular with frequent mitotic figures (Fig. 9*F*, *arrow*).

MV-CEA Causes No Neurotoxicity after Intracerebral Administration in MV-susceptible Ifnar^{ko} CD46 Ge Transgenic Mice. To evaluate toxicity to normal brain, resulting from intracranial administration of MV-CEA, we used the transgenic mouse model Ifnar^{ko} CD46 Ge. These mice are IFN-$\alpha\beta$ receptor knockout, express CD46 receptor, and, as described in the method section, are susceptible to MV replication.

MV-CEA was administered at the same dose, volume, and schedule as for the orthotopic efficacy study, using the same stereotactic parameters. Treated mice were observed up to 3 weeks after the last MV-CEA administration before being euthanized. UV light-inactivated MV-CEA-treated mice and normal saline-treated mice were included as controls. At no point during the course of the experiment was neurological or other clinical toxicity observed. Treated mice continued to thrive and maintained the same activity level. Mice were euthanized at 2–4, 14, and 21 days after the last MV-CEA injection to assess for acute, subacute, and late toxicity. Pathologic examination of the brains of the control mice (both UV MV-CEA- and normal saline-injected) revealed reactive changes at the injection site, mainly consisting of macrophages (Fig. 10, *A* and *B*). Pathologic examination of the brains of the MV-CEA-treated mice revealed reactive changes surrounding the injection scar with a more evident microglial reaction (Fig. 10, *C* and *D*) and occasional microglial nodules near the injection area (Fig. 10, *E* and *F*). When specimens corresponding to early (day 2–4) *versus* intermediate (day 14) *versus* late (day 21) time points after completion of injection were examined comparatively,

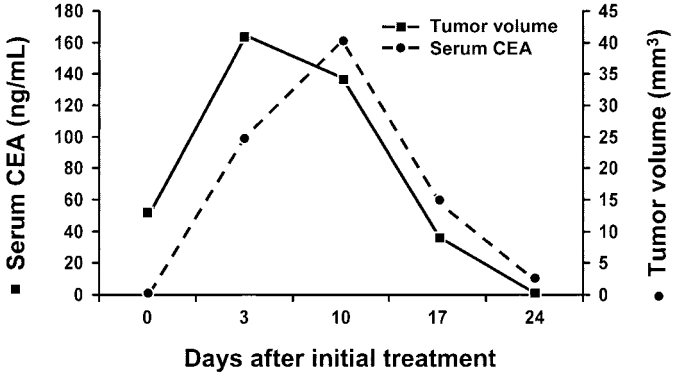

Fig. 7. Serum CEA plotted with U87 subcutaneous tumor volume in BALB/c nude mice treated with i.v. MV-CEA. The rise and fall of serum CEA parallel the growth and regression of the tumor.

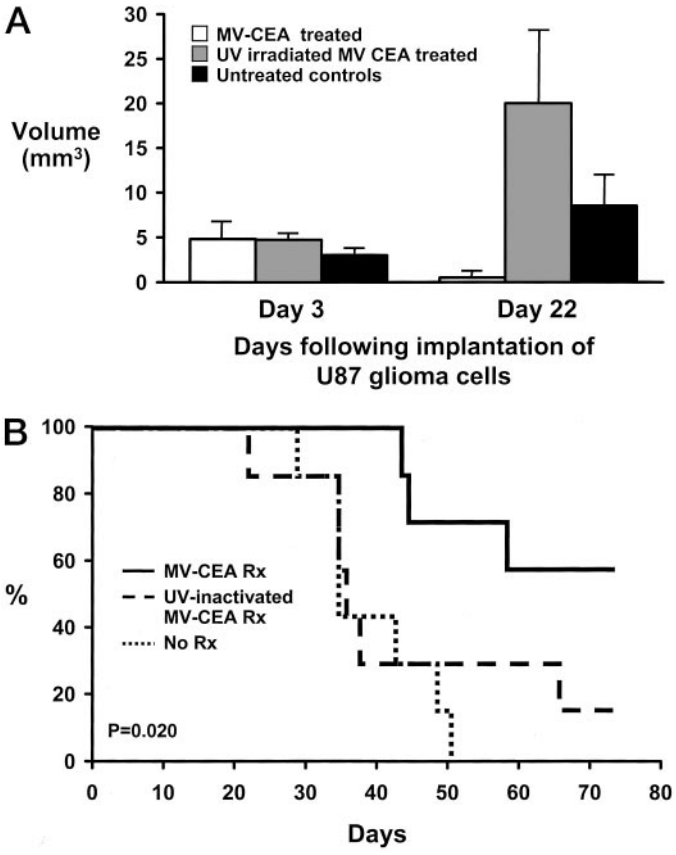

Fig. 8. *A*, antitumor effect of MV-CEA, administered intratumorally in an orthotopic U87 tumor model. Tumors were established by injection of 10^6 U87 cells into the right caudate nucleus of BALB/c nude mice. The intracranial tumor volume was measured by MRI 3 days after tumor cell implantation (before initiating treatment) and again after treatment completion, 21 days from tumor implantation. Mice were randomly assigned to either MV-CEA treatment (3×10^5 pfu/dose for 6 doses), UV-inactivated MV-CEA treatment (3×10^5 pfu/dose for 6 doses), or remained untreated. The intracranial volumes were similar between the three groups before initiating treatment ($P = 0.28$). There was significant tumor regression in the mice treated with MV-CEA as compared with the two other groups ($P = 0.0028$). The tumor volumes between the mice treated with UV inactivated MV-CEA and untreated mice were similar ($P = 0.26$). *B*, significant prolongation of survival is seen in the mice treated with MV-CEA as compared with the mice that received UV-inactivated MV-CEA or no treatment ($P = 0.02$).

there was no evidence of progression of the glial infiltrate. Furthermore, the neurons appeared normal and there was no evidence of necrosis or meningitis. In addition, no pathologic changes in the contralateral hemisphere were observed. Repeat blood sampling of the treated animals failed to detect CEA elevation.

DISCUSSION

Gliomas represent excellent targets for gene transfer approaches because of their limited ability to metastasize. However, despite being the first human malignancy targeted by gene transfer approaches since the early 1990s, clinical trials in gliomas were significantly hampered by lack of efficacy (5, 30). A gap exists between the efficacy of the therapeutic genes in preclinical models and the lack of antitumor activity observed in clinical trials. The low transduction efficiency of replication-defective viral vectors appears to present a significant hindrance to effective treatment. Replication-competent viral vectors are a possible solution to this problem.

The first replicating virus used in a clinical trial for treatment of brain tumors was G207, a double HSV-1 mutant that, unlike wild-type HSV-1, replicates poorly in neural tissue. The patients in this trial received between 10^6 and 10^9 pfu of G207. No encephalitis or other long-term toxicity attributed the treatment were observed. The study was not designed to evaluate *in vivo* replication of the virus, as tumor specimens were not obtained after virus inoculation, thus pointing to inherent difficulties in assessing the potential of viral therapies in brain tumor patients (31). Another Phase I study using conditionally replicating HSV in nine patients with malignant glioma obtained similar safety data with doses up to 10^5 pfu (32). No objective clinical responses were observed in any of these Phase I clinical trials, although antitumor activity was a secondary endpoint. Other replicating viruses such as ONYX-015 and reovirus are also currently in clinical testing.

There are two characteristics of MV-CEA that make it worth additional exploring in the treatment of gliomas. The agent has significant antitumor activity as demonstrated by the CPE of MV-CEA on malignant glioma cell lines *in vitro*, and its efficacy in subcutaneous and intracranial orthotopic models. As Figs. 2 and 3 demonstrate, MV-CEA, even in very low MOI, has a significant CPE against a variety of glioblastoma cell lines. At an MOI of 1, complete eradication of monolayer cultures of U87, U118, and U251 cells was observed at 72–96 h. Complete tumor regression was seen in all of the

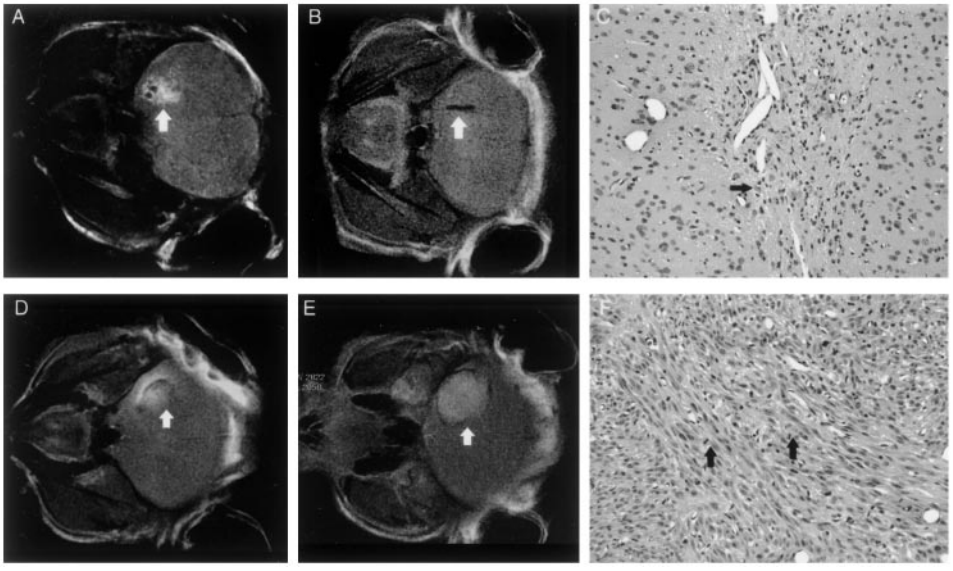

Fig. 9. *A–F*, magnetic resonance image of the brain before (*A*) and 18 days after initiation of treatment (*B*) in a mouse treated intratumorally with MV-CEA (total dose 1.8×10^6 pfu). There is complete regression of the treated tumor. The remnant of a needle track is seen at the site of the tumor implant but there is no evidence of residual tumor. Brain section from the same mouse (H&E stain) demonstrated no residual tumor (*C;* ×200). The needle track (*arrow*) seen on the MRI in *B* is evident. In addition, there is evidence of glial scar, cholesterol clefts, and hemosiderin laden macrophages (*arrows*). No tumor cells are present. Magnetic resonance image of a mouse brain before (*D*) and 18 days after initiation of treatment (*E*) in a mouse treated intratumorally with UV-inactivated MV-CEA (total dose 1.8×10^6 pfu) reveals significant tumor growth. Histological section from the mouse's brain (H&E stain) reveals a hypercellular U87 tumor with frequent mitotic figures (*arrow*) (*F;* ×200 magnification).

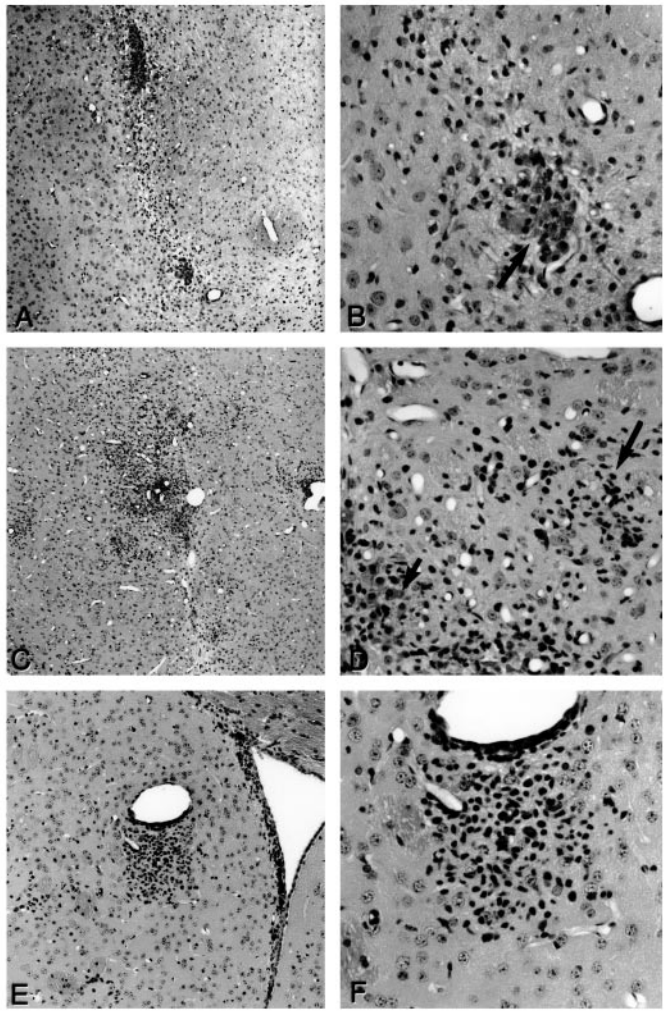

Fig. 10. *A–F*, histological examination of Ifnar^{ko} CD46 Ge mouse brain after administration of UV-inactivated MV-CEA (*A* and *B*) or MV-CEA (*C–F*). Minimal reaction is observed at the injection site after administration of UV-inactivated MV-CEA (*A* and *B*). An injection track is identified (*A;* ×100) with reactive changes, mainly macrophages with foamy cytoplasm (*arrow; C,* ×400). Administration of MV-CEA resulted in reactive changes (*C,* ×100) and a more evident microglial reaction (*arrow*) in addition to macrophages (*small arrow*) limited to the site of injection (*D,* ×400), with occasional microglial nodules (*E,* ×100; *F,* ×400). There were no distal changes, no necrosis, and no meningeal inflammation.

MV-CEA-treated mice in the subcutaneous U87 model and 7 of 8 mice in the intracranial model. Significant prolongation of survival was also seen in both animal models (Figs. 6 and 8). Our data demonstrate the significant therapeutic potential of MV-CEA against malignant gliomas. Furthermore, serum CEA levels represented a good correlate of viral gene expression *in vivo* (Fig. 7) and correlated with viral replication *in vitro* (Fig. 3). Detection of CEA in the serum is widely available and can become a cost-effective method of monitoring the viral gene expression, that also allows repeated measurements to be obtained with minimal risk to the patient.

The ability to track gene expression and its variation over time in the individual patient is important for optimizing viral/gene therapy. Development of methodology for noninvasive monitoring of gene expression during treatment is particularly pertinent in clinical trials for treatment of brain tumors, because the invasive alternative, *i.e.,* obtaining consecutive tumor biopsies, has significant inherent risks.

Other approaches to noninvasive monitoring of gene transfer use imaging modalities such as PET and SPECT. Noninvasive localization of gene expression (molecular imaging) using these modalities relies on the transduction of marker genes that encode enzymes or receptors, which leads to a regional accumulation of radiolabeled marker substrates or receptor binding compounds. These substrates can then be detected by radionuclide imaging. [^{124}I]-FIAU, a specific substrate for HSV-1 thymidine kinase, and PET have been used for the noninvasive localization of retroviral, adenoviral, and herpes simplex viral vector-mediated HSV-1-thymidine kinase gene expression in rodents (33–36). The same radioisotope and PET imaging was used in five patients in a Phase I/II clinical trial of IT infusion of the cationic liposomal vector DAC-30, encoding HSV-tk in patients with recurrent glioblastomas (37). In only one of five patients [^{124}I]-FIAU accumulation in the infusion site was noted, indicating that a critical number of tk-gene transduced tumor cells per voxel had to be present in order for the PET scanner to detect FIAU accumulation. These results also point to the fact that improving on sensitivity of PET scanning detection will be necessary for this technology to be a helpful guidance for management of patients in gene transfer trials. Another potential limitation related to the use of PET for gene transfer imaging is that only a few specialized centers can produce the necessary isotopes and that the number of PET scans that can be performed during gene therapy is limited because of radiation safety considerations. SPECT imaging uses a different radioactive label, [^{131}I]FIAU, as a substrate for phosphorylation by HSV-tk. Tjuvajev *et al.* (38) showed that the areas of radioactivity on the SPECT image corresponds to the areas of HSV-tk gene expression in rats bearing mammary carcinoma tumors. The technology required for SPECT is more widely available than PET; however, SPECT imaging has poorer spatial resolution than PET.

Whereas our CEA expression monitoring strategy does not provide information regarding location of transgene expression, it is far more convenient and inexpensive than expression monitoring with PET or SPECT tracers. Serum CEA monitoring can be performed as frequently as necessary and it can provide a real-time assessment of viral replication with minimal risk to the patient, thus allowing individualization of dosing both from a standpoint of safety and efficacy. For example, if therapeutic administration of MV-CEA results in a flat CEA curve, this would signal the need for repeat higher dosing to achieve viral replication and antitumor efficacy. On the other hand, in an ideal therapeutic case scenario, we would expect to observe similar CEA curves as for the MV-CEA-treated group in our study: CEA titers increase as the virus replicates in the tumor cells. After tumor cell death and tumor regression, the viral replication stops and CEA titers return to normal. Furthermore, CEA detection represents a very sensitive means of following viral gene expression, because viral replication even in very small intracranial tumors could lead in serum CEA elevation.

The mechanism of cell death in glioma cell lines after infection with MV-CEA is predominantly apoptotic. These results are in agreement with prior work indicating that apoptosis is the main mechanism of death for MV-induced syncytia (39). Similarly, using a variety of techniques including TUNEL assay, DNA ladders, and real-time microscopy we have demonstrated extensive apoptosis after transfection of glioma cell lines with DNA coding for fusogenic MV membrane glycoproteins F and H (6).

Attenuated strains of the Edmonston vaccine lineage of MV has been used in vaccines for many years with an excellent safety record. Testing of vaccine strains by intracerebral administration to susceptible primates represents an additional safeguard to ensure lack of neurotoxicity, the latter being especially pertinent if IT administration of MV-CEA is contemplated in patients with recurrent gliomas. In animal work performed in the early 1970s, Albrecht *et al.* (40) found no clinical signs of encephalitis in rhesus monkeys that were inoculated in the right thalamus with low-passage wild Edmonston or

attenuated Schwartz strains of MV. Although MV was isolated from 4 of the 12 animals when sections of their brains were cultured with Vero cells, there was no histological evidence of active measles infection such as intranuclear inclusions in the brains of the monkeys. Administration of an attenuated Edmonston strain of MV ($10^{2.75}$ pfu/0.1 ml) to grivet monkeys both intrathalamically (0.5 ml/thalamus) and intracisternally (0.2 ml) had no clinical toxicity, and resulted in pathologic changes (gliosis with mixed cellular infiltrate) that were not different from the ones observed in animals injected with vehicle control (41). Similarly, infracerebral inoculation of an attenuated strain of MV ($10^{1.8}$-$10^{3.5}$ pfu/ml) in the cerebral hemisphere (0.5 ml) and cisterna magna (0.25) of cynomologous monkeys had no clinical toxicity. No virus was isolated from the cerebrospinal fluid, and no changes compatible with viral injury were observed at postmortem 21 days after viral inoculation (42). The MV strain of the Edmonston vaccine lineage that we used in our studies is additionally attenuated by the insertion of the CEA gene in frame in position one. To further investigate the selectivity/toxicity issue, we administered MV-CEA intracerebrally in Ifnar^{ko} CD46 Ge mice, using the same dose and stereotactic parameters as for the efficacy study. In this mouse strain, which is susceptible to MV replication (26), we observed no neurological or other clinical toxicity. Furthermore, detailed histopathologic examination of the brain at different time points up to day 21 after completion of the viral injections revealed focal infiltration with microglial cells in proximity to the injection tract, but no evidence of encephalitis or necrosis. In addition, no histopathologic changes outside the injected caudate nucleus were observed. These data point toward the safety of the proposed approach. Nevertheless, additional studies in primates will likely be necessary before translating this approach to the clinic.

In conclusion, we have shown that MV-CEA has potent therapeutic efficacy against gliomas in both subcutaneous and intracranial orthotopic mouse models. Tracking of viral gene expression can be easily and safely performed by measuring serum CEA. Thus, monitoring serum CEA levels can allow for individualization of dose in a clinical setting without a need for repeat brain biopsies. Our results set the foundation for additional studies in preparation for using MV-CEA in a clinical trial for treatment of glioblastoma multiforme.

ACKNOWLEDGMENTS

We thank Dr. Roberto Cattaneo for the Ifnar^{ko} CD46 Ge mice, Dr. V. Shane Pankratz for the statistical analysis, and Raquel Ostby for help with preparation of the manuscript.

REFERENCES

1. Greenlee, R., Murray, T., Bolden, S., and Wingo, P. Cancer statistics. CA Cancer J. Clin., *50:* 7–33, 2000.
2. Berger, M., Prados, M., and van Gilder, J. Phase II trial of GLI 328 HSV-tk gene therapy in recurrent glioblastoma. Cancer Gene Ther., *4*(Suppl.)*:* 542, 1997.
3. Oldfield, E. Gene therapy for the treatment of brain tumors using intratumoral transduction with the thymidine kinase gene and intravenous gancyclovir. Hum. Gene Ther., *4:* 39–69, 1993.
4. Rainov, N. A phase III clinical evaluation of herpes simplex virus type 1 thymidine kinase and gancyclovir gene therapy as an adjuvant to surgical resection and radiation in adults with previously untreated glioblastoma multiforme. Hum. Gene Ther., *11:* 2389–2401, 2000.
5. Ram, Z., Culver, K., Oshiro, E., *et al.* Therapy of malignant brain tumors by intratumoral implantation of retroviral vector-producing cells. Nat. Med., *3:* 1354–1361, 1997.
6. Galanis, E., Bateman, A., and Johnson, K. Use of viral fusogenic membrane glycoproteins as novel therapeutic transgenes in gliomas. Hum. Gene Ther., *12:* 811–821, 2001.
7. Lang, F. F., Fuller, G. N., Prados, M., and Yung, W. A. Preliminary results of a phase I clinical trial of adenovirus-mediated p53 gene therapy for recurrent gliomas: Biological studies. Proc. Am. Soc. Clin. Oncol., *19:* 455a, 2000.
8. Wild, T., Malvoisin, E., and Buckland, R. Measles virus: both the hemagglutinin and fusion glycoproteins are required for fusion. J. Gen. Virol., *72(part 2):* 439–442, 1991.
9. Tatsuo, H., Ono, N., Tanaka, K., *et al.* SLAM (CDw150) is a cellular receptor for measles virus. Nature (Lond.), *406:* 893–897, 2000.
10. Dorig, R., Marcil, A., Chopra, A., *et al.* The human CD46 molecule is a receptor for measles virus (Edmonston strain). Cell, *75:* 295–305, 1993.
11. Naniche, D., Varior-Krishnan, G., Cervoni, F., *et al.* Human membrane cofactor protein (CD46) acts as a cellular receptor for measles virus. J. Virol., *67:* 6025–6032, 1993.
12. Jurianz, K., Ziegler, S., Garcia-Schuler, H., *et al.* Complement resistance of tumor cells: basal and induced mechanisms. Mol Immunol, *36:* 929–939, 1999.
13. Cutts, F. T., Markowitz, L. E. Successes and failures in measles control. J. Infect. Dis., *170*(Suppl. 1)*:* S32–S41, 1994.
14. Grote, D., Russell, S., and Cornu, T. Live attenuated measles virus induces regression of human lymphoma xenografts in immunodeficient mice. Blood, *97:* 3746–3754, 2001.
15. Peng, K. W., Ahmann, G. J., Pham, L., *et al.* Systemic therapy of myeloma xenografts by an attenuated measles virus. Blood, *98:* 2002–2007, 2001.
16. Peng, K. W., TenEyck, C. J., Galanis, E., *et al.* Intraperitoneal therapy of ovarian cancer using an engineered measles virus. Cancer Res., *62:* 4656–4662, 2002.
17. Yanagi, Y. The cellular receptor for measles virus. Uirusu, *51:* 201–208, 2001.
18. Schneider, U., von Messling, V., Devaux, P., *et al.* Efficiency of measles virus entry and dissemination through different receptors. J. Virol., *76:* 7460–7467, 2002.
19. Berinstein, N. L. Carcinoembryonic antigen as a target for therapeutic anticancer vaccines: a review. J. Clin. Oncol., *20:* 2197–2207, 2002.
20. Peng, K. W., Facteau, S., Wegman, T., *et al.* Non-invasive *in vivo* monitoring of trackable viruses expressing soluble marker peptides. Nat. Med., *8:* 527–531, 2002.
21. Radecke, F., Spielhofer, P., Schneider, H., *et al.* Rescue of measles virus from cloned DNA. EMBO J., *14:* 5773–5784, 1995.
22. Spearman, C. The method of right and wrong cases without Gauss's formula. Br. J. Psychol., *2:* 227–242, 1908.
23. Cathomen, T., Naim, H., and Cattaneo, R. Measles virus with altered envelope protein cytoplasmic tails gain cell fusion competence. J. Virol., *73:* 9568–9575, 1998.
24. Dethlefsen, L., Prewitt, J., and Mendelsohn, M. Analysis of tumor group curves. J. Natl. Cancer Inst., *40:* 389–405, 1968.
25. Rencher, A. C. Methods of Multivariate Analysis, Ed. 2. New York: John Wiley & Sons, 2002.
26. Mrkic, B., Pavlovic, J., Rulicke, T., *et al.* Measles virus spread and pathogenesis in genetically modified mice. J. Virol., *72:* 7420–7427, 1998.
27. Roscic-Mrkic, B., Schwendener, R. A., Odermatt, B., *et al.* Roles of macrophages in measles virus infection of genetically modified mice. J. Virol., *75:* 3343–3351, 2001.
28. Mrkic, B., Odermatt, B., Klein, M. A., *et al.* Lymphatic dissemination and comparative pathology of recombinant measles viruses in genetically modified mice. J. Virol., *74:* 1364–1372, 2000.
29. Singh, M., Cattaneo, R., and Billeter, M. A. A recombinant measles virus expressing hepatitis B virus surface antigen induces humoral immune responses in genetically modified mice. J. Virol., *73:* 4823–4828, 1999.
30. Shand, N., Weber, Mariani, L. *et al.* A phase 1–2 clinical trial of gene therapy for recurrent glioblastoma multiforme by tumor transduction with the herpes simplex thymidine kinase gene followed by ganciclovir. GLI328 European-Canadian Study Group. Hum. Gene Ther., *29, 10:* 2325–2335, 1999.
31. Markert, J., Medlock, M., Rabkin, S., *et al.* Conditionally replicating herpes simplex virus mutant. G207 for the treatment of malignant glioma: results of a phase I trial. Gene Ther., *7:* 867–874, 2000.
32. Rampling, R., Cruickshank, G., Papanastassious, V., *et al.* Toxicity evaluation of replication-competent herpes simplex virus (ICP 34.5 null mutant 1716) in patients with recurrent malignant glioma. Gene Ther., *7:* 859–866, 2000.
33. Blasberg, R., and Tjuvajev, J. Herpes simplex virus thymidine kinase as a marker/reporter gene for PET imaging of gene therapy. Q. J. Nucl. Med., *43:* 163–169, 1999.
34. Gambhir, S., Herschman, H., Cherry, S., *et al.* Imaging transgene expression with radionuclide imaging technologies. Neoplasia, *2:* 118–138, 2000.
35. Bennett, J., Tjuvajev, J., Johnson, P., *et al.* Positron emission tomography imaging for herpes virus infection: implications for oncolytic viral treatments of cancer. Nat. Med., *7:* 859–863, 2001.
36. Jacobs, A., Tjuvajev, J., Dubrovin, M., *et al.* Positron emission tomography-based imaging of transgene expression mediated by replicating-conditional, oncolytic herpes simplex virus type 1 mutant vectors *in vitro*. Cancer Res., *61:* 2983–2995, 2001.
37. Jacobs, A., Voges, J., Reszka, R., *et al.* Positron-emission tomography of vector-mediated gene expression in gene therapy for gliomas. Lancet, *358:* 727–729, 2001.
38. Tjuvajev, J., Finn, R., Watanabe, K., *et al.* Noninvasive imaging of herpes virus thymidine kinase gene transfer and expression: a potential method for monitoring clinical gene therapy. Cancer Res., *56:* 4087–4095, 1996.
39. Esolen, L. M., Park, S. W., Hardwick, J. M., *et al.* Apoptosis as a cause of death in measles virus-infected cells. J. Virol., *69:* 3955–3958, 1995.
40. Albrecht, P., Shabo, A., Burns, R., *et al.* Experimental measles encephalitis in normal and cyclophosphamide treated rhesus monkeys. J Infect. Dis., *126:* 154–161, 1972.
41. Buynak, E. B., Peck, H. M., Creamer, V. M. D., Goldner, H., and Hilleman, M. R. Differentiation of virulent from avirulent measles strains. Am. J. Dis. Child, *103:* 460–473, 1962.
42. Enders, J. F., Katz, S. L., Milovanovic, M. V., and Holloway, A. Studies of an attenuated measles-virus vaccine. Development and preparation of the vaccine: Technics for assay of effects of vaccination. N. Engl. J. Med., *263:* 153–159, 1960.